PROCEEDINGS OF SCIENCE

Top physics measurements at LHCb

Stephen Farry[*†]
University of Liverpool
E-mail: stephen.farry@cern.ch

LHCb, while purpose built for b-physics, also functions as a general purpose forward detector, covering the pseudo-rapidity range 2.0 to 5.0. LHCb has measured forward top production using final states accessible from both single top and top pair production processes. Measurements in the LHCb acceptance have particular sensitivity to high and low values of Bjorken-x when compared to other LHC measurements, and consequently offer complementary constraints on Bjorken-x. A selection of LHCb results in this area are presented.

The European Physical Society Conference on High Energy Physics
5-12 July, 2017
Venice

[*]Speaker.
[†]on behalf of the LHCb collaboration.

PoS(EPS-HEP2017)440

1. Introduction

The LHCb experiment [1] is a dedicated forward detector at the LHC, fully instrumented in the pseudorapidity region $2.0 < \eta < 5.0$. It has been optimised to identify and reconstruct b and c hadron decays through precision tracking, vertexing and particle identification. These properties make LHCb ideally suited to perform the tagging of heavy flavour jets, which can be used to identify and measure the production of top quarks in the forward region. Such a measurement, originally proposed in order to measure asymmetries in $t\bar{t}$ production [2], also has the potential to reduce the uncertainties on the gluon PDF by up to 20% at large-x [3]. As the LHCb experiment collects a lower rate of luminosity than the ATLAS and CMS experiments, and has a smaller fiducial acceptance, a lower number of top quark events are expected to be produced at LHCb. Measurements of top quark production have been performed at LHCb in Run I in two different final states, the μb final state, containing a muon and a b-tagged jet, and the ℓbb final state, containing a muon or electron in addition to two b-jets. The heavy flavour tagging techniques used at LHCb are described first, before each measurement is presented in turn.

2. Jet Reconstruction and Heavy Flavour Tagging

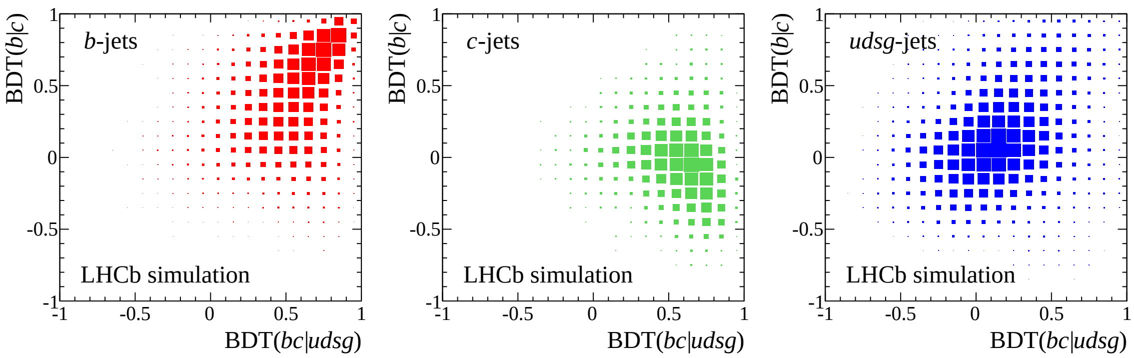

Figure 1: A two-dimensional representation of the BDT responses in simulation is shown for (left) b-jets, (middle) c-jets and (right) light-jets.

Jet reconstruction at LHCb is performed by first preparing the inputs using a particle flow algorithm as described in [4], and then clustering the jets using an anti-k_{T} algorithm with distance parameter, $R = 0.5$. Heavy flavour tagging is performed using the secondary vertex (SV) tagging algorithm outlined in [5]. The tagging first searches for an SV within the jet which satisfies specific track and vertex quality requirements. Two boosted decision trees (BDTs) are then trained on simulated b, c, and light jet samples using properties of the SV and the jet in order to separate light jets from heavy quark jets (BDT($bc|udsg$)), and $b-$jets from $c-$jets (BDT($b|c$)). The primary variables used are related to the $b-$ or $c-$hadron decay as these are expected to be well modelled in simulation. One parameter used to discriminate the jet types is the corrected mass, M_{cor}, defined as

$$M_{\mathrm{cor}} = \sqrt{M^2 + p^2 \sin^2\theta} + p\sin\theta$$

PoS(EPS-HEP2017)440

where M and p are the mass and momentum of the particles that form the SV and θ is the angle between the path joining the primary vertex and the SV, and the combined momentum of the particles forming the SV. It represents the minimum mass the long-lived object decaying at the vertex can have which is consistent with the flight direction. A two-dimensional representation of the BDT responses for b, c and light jets is shown in Figure 1. Where requirements are placed on the BDT($bc|udsg$) response, the tagging efficiency versus light jet mis-tag rate is shown for b and $c-$jets in Figure 2.

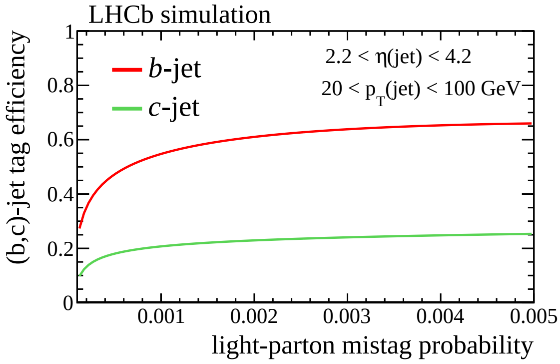

Figure 2: The efficiency for tagging b and $c-$jets versus the mis-tag probability for light jets obtained from simulation.

3. Top production in the μb final state

The measurement of top production in the μb final state is performed using data collected at centre-of-mass energies of 7 and 8 TeV, corresponding to integrated luminosities of approximately 1 and 2 fb^{-1} respectively [6]. The selection is based on previous studies of W production in association with b and $c-$jets performed at LHCb using the same dataset [7]. Events are selected which contain a muon with a transverse momentum, $p_{\mathrm{T}}(\mu)$, of greater than 25 GeV in the pseudorapidity region $2 < \eta < 4.5$, in addition to a jet with a transverse momentum, $p_{\mathrm{T}}(j)$, satisfying $50 < p_{\mathrm{T}}(j) < 100$ GeV in the pseudorapidity range $2.2 < \eta < 4.2$. The muon and the jet are also required to be "unbalanced" in p_{T} by requiring that $p_{\mathrm{T}}(j_\mu + j)$, representing the p_{T} of the vectorial sum of j_μ and j, is greater than 20 GeV, where j_μ is a reconstructed jet containing the muon candidate and j is the associated jet. The observable is expected to be large for W+jet events due to the missing neutrino in the final state and small for mis-identified QCD di-jet production where the jet momenta are balanced.

The purity is determined using a template fit to the isolation variable $p_{\mathrm{T}}(\mu)/p_{\mathrm{T}}(j_\mu)$, where $p_{\mathrm{T}}(\mu)$ is the transverse momentum of the muon in the final state, and $p_{\mathrm{T}}(j_\mu)$ is the transverse momentum of j_μ. This variable is expected to peak towards unity for signal events, and to be spread to lower values for backgrounds arising from QCD multi-jet processes. The electroweak template shapes are taken from simulation and corrected for differences between data and simulation while the QCD background is estimated using a data-driven method. In each bin of $p_{\mathrm{T}}(\mu)/p_{\mathrm{T}}(j_\mu)$, the contribution from b-jets is extracted by requiring that the jets contain an SV and performing a template fit to the resultant two-dimensional BDT distributions. The fits are performed separately for positive and negative muons, and for the different centre-of-mass energies.

The significance of the top quark contribution to the selected data sample is determined by comparing the observed event yield and charge asymmetry of Wb production to the SM prediction with and without the contribution from top quark production. The predictions are calculated at NLO in perturbative QCD using the MCFM generator and folded for detector effects. The observed event yield and charge asymmetry are shown in Figure 3. The statistical significance of the top quark contribution is calculated using a binned profile likelihood test to compare the data to the SM hypothesis without a top quark contribution and where contributions from both single top and $t\bar{t}$ production are included. The significance obtained is 5.4σ using Wilks' theorem, confirming the observation of top quark production in the forward region.

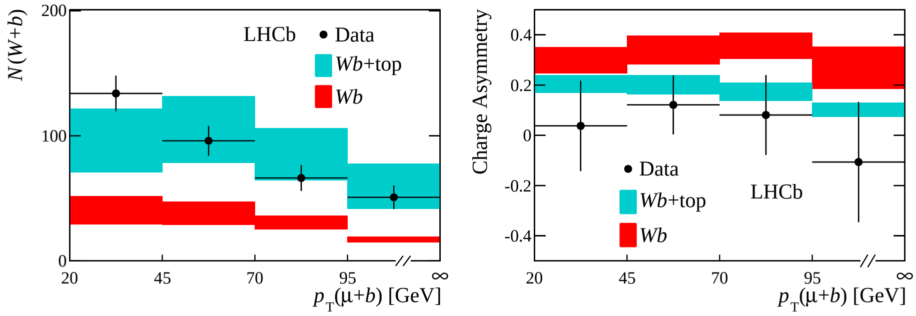

Figure 3: The observed (left) event yield and (right) charge asymmetry of Wb production compared to SM predictions calculated with and without the contribution from top quark production.

4. Top production in the ℓbb final state

A simultaneous measurement of $W + c\bar{c}$, $W + b\bar{b}$ and $t\bar{t}$ production is performed at LHCb in the ℓbb final state using 2 fb^{-1} of data collected at a centre-of-mass energy of 8 TeV [8]. Events are selected which contain either a muon or electron with a transverse momentum in excess of 20 GeV in the pseudorapidity region between 2.0 and 4.5(4.25) for muons (electrons). Two jets are also required to be present with transverse momentum greater than 12.5 GeV in the pseudorapidity range $2.2 < \eta < 4.2$. The jets are further required to be SV-tagged and to satisfy BDT$(bc|udsg) > 0.2$. The leptons and jets are required to be separated by a distance of 0.5 in $(\eta - \phi)$ space and the transverse component of the vector sum of the momentum of the lepton and the two jets is required to be greater than 15 GeV. The data is split into four sub-samples by the flavour and charge of the lepton and a simultaneous fit is performed to four variables in order to determine the $W + c\bar{c}$, $W + b\bar{b}$ and $t\bar{t}$ signal yields. The four variables used in the fit are: the invariant mass of the di-jet system; the output of a multivariate classifier designed to separate $t\bar{t}$ and $W + b\bar{b}$ events using a uniform gradiant boosting technique [9] (uGB); and the output of BDT$(b|c)$ for both jets. The expected backgrounds from electroweak processes, such as $Z + b\bar{b}$, $Z + c\bar{c}$ and single top production, are fixed to the NLO predictions obtained from MCFM, while the QCD background is normalised using a data-driven method. The result of the simultaneous 4D-fit in the μ^+ sample is shown as a

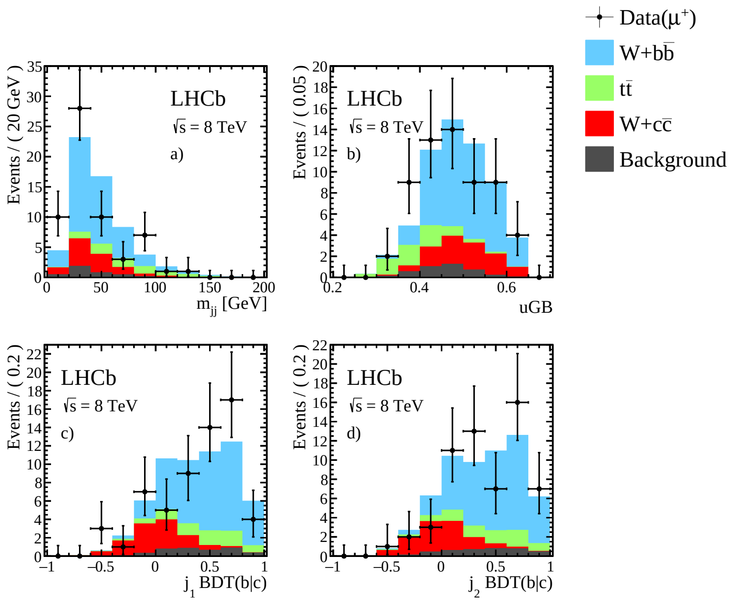

Figure 4: Projections of the simultaneous 4D-fit results for the μ^+ sample.

projection on each of the four fit variables in Fig. 4. The significance of the $t\bar{t}$ signal is determined using Wilks' theorem to be 4.9σ, and the extracted cross-section is in agreement with Standard Model predictions. The measurement has also been reinterpreted as limits on Higgs production in association with a W or Z boson in the forward region [10].

5. Conclusion

Measurements of top quark production at LHCb are presented in the μb and ℓbb final states, with observed significances of 5.4 and 4.9σ respectively. The resulting cross-sections are found to be in good agreement with SM predictions. While the measurements are currently statistically limited, a significant increase in the top quark production cross-section is expected in Run-II at the higher centre-of-mass energy of 13 TeV. In addition to the increased statistical precision available for the final states presented here, other final states will become statistically accessible and allow a higher purity and precision to be achieved in top physics measurements at LHCb.

References

[1] LHCb collaboration, JINST **3**, p. S08005 (2008).
[2] A. L. Kagan, J. F. Kamenik, G. Perez, and S. Stone, Phys. Rev. Lett. **107**, p. 082003Aug (2011).
[3] R. Gauld, JHEP **02**, p. 126 (2014), arXiv:1311.1810 [hep-ph] .
[4] LHCb collaboration, JHEP **01**, p. 033 (2014), arXiv:1310.8197 [hep-ex] .
[5] LHCb collaboration, JINST **10**, p. P06013 (2015), arXiv:1504.07670 [hep-ex] .
[6] LHCb collaboration, Phys. Rev. Lett. **115**, p. 112001 (2015), arXiv:1506.00903 [hep-ex] .
[7] LHCb collaboration, Phys. Rev. **D92**, p. 052001 (2015), arXiv:1505.04051 [hep-ex] .
[8] LHCb collaboration, Phys. Lett. **B767**, 110–120 (2017), arXiv:1610.08142 [hep-ex] .
[9] A. Rogozhnikov *et al.*, JINST **10**, p. T03002 (2015), arXiv:1410.4140 [hep-ex] .
[10] LHCb collaboration, "LHCb-CONF-2016-006," Sep (2016).

PoS(EPS-HEP2017)440